Supporting Information for

Type-II GaSe/MoS_2 van der Waals Heterojunction for High-performance Flexible Photodetector

Shuai Wang [‡1], Xiaoqiu Tang [‡1], Ezimetjan Alim [1], Xingdong Sun [1], Zheng Wei *[1], Hualong Tao [1], Yang Wen [1], Sumei Wu [1], Yongqing Cai [2], Yingying Wang [3], Yao Liang [1] and Zhihua Zhang [1]

[1] School of Materials Science and Engineering, Dalian Jiaotong University, Dalian 116028, China

[2] Shenzhen Institute for Quantum Science and Engineering, Southern University of Science and Technology, Shenzhen 518055, China

[3] Department of Optoelectronic Science, Harbin Institute of Technology at Weihai, Weihai 264209, China

* Correspondence: zhengwei@djtu.edu.cn

‡These authors contributed equally to this work.

(1) Structure and energy spectrum characterization of the GaSe/MoS_2 heterojunction

To discern the fine morphology characterization and elemental composition analysis of the GaSe/MoS_2 van der Waals heterojunction, we have provided the TEM, HRTEM and EDS mapping images of the sample. Figure S1(a) presents the TEM image of the GaSe/MoS_2 van der Waals heterojunction with GaSe on the lower layer and MoS_2 on the upper layer, and the dotted line indicates the edge of MoS_2. It is obvious that the sample shows a clean surface and sharp interface. The HRTEM image of the heterojunction region is shown in Figure S1(b) and the Moire patterns are clearly visible. Figure S1(c-f) are the EDS mapping images of the GaSe/MoS_2 van der Waals heterojunction in Figure S1(a). The signals of the S and Mo elements are detected in the MoS_2 region and the Se and Ga elements appear in the entire area of the sample, which is in accordance with the structure of the heterojunction.

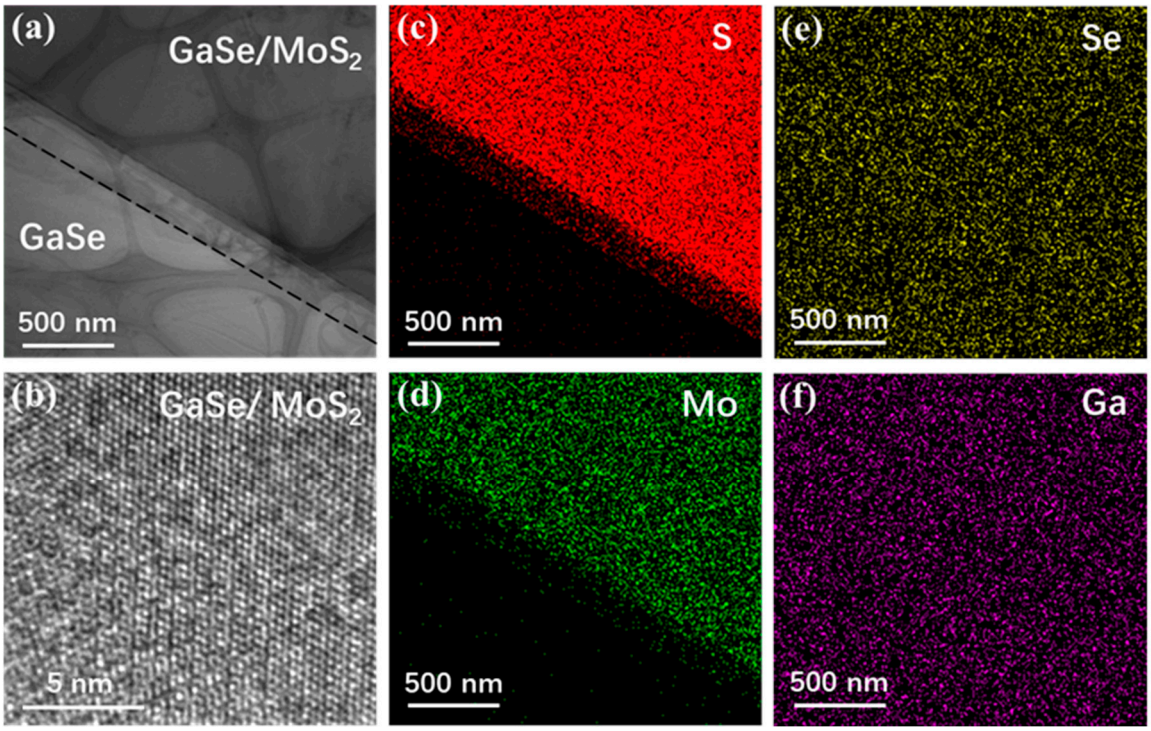

Figure S1. Structure and energy spectrum characterization of the GaSe/MoS_2 van der Waals heterojunction. (a,b) TEM and HRTEM images of the GaSe/MoS_2 van der Waals heterojunction, respectively. (c-f) EDS mapping images of the GaSe/MoS_2 van der Waals heterojunction.

(2) Crystal structures and energy-band diagrams of MoS_2 and GaSe

The schematic diagrams of the MoS_2 and GaSe crystal structures are illustrated in Figure S2(a). Monolayer MoS_2 and GaSe are formed by vertically stacked S-Mo-S atomic layers and Se-Ga-Ga-Se atomic layers, respectively, while the bulk crystals are composed of vertical stacking of their monolayers with vdW force between the interfaces. The energy-band diagrams of separated MoS_2 and GaSe are presented in Figure S2(b). E_0, E_C and E_V denote the vacuum energy level, minimum conduction band and maximum valence band, respectively. The electron affinity of MoS_2 is ~ 4.1 eV, whereas that of GaSe is ~ 2.8 eV [1,2]. The valence band maximum of MoS_2 is 0.5 eV lower than that of GaSe, which indicates that the vertically stacked GaSe/MoS_2 vdW heterostructure generates a type-II band alignment, with the minimum conduction band corresponding to MoS_2 and the maximum valence band corresponding to GaSe.

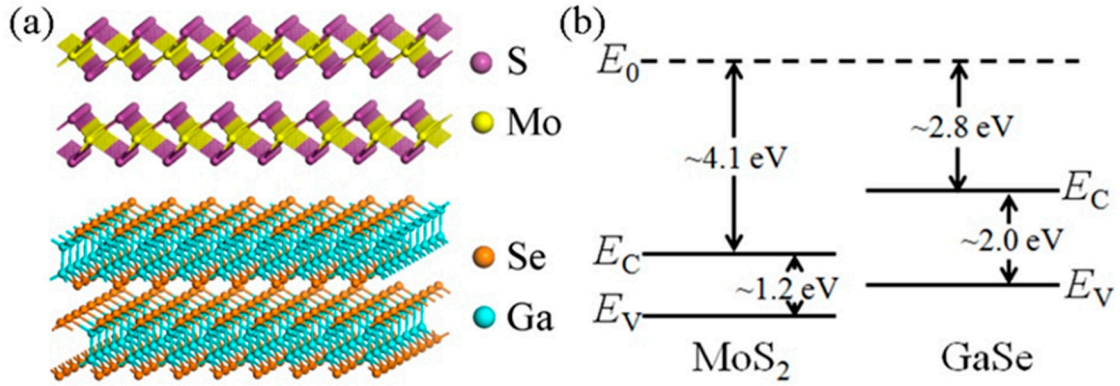

Figure S2. Crystal structures and energy-band diagrams of separated MoS_2 and GaSe. (a) Schematic diagrams of MoS_2 and GaSe crystal structures. (b) Energy-band diagrams of separated MoS_2 and GaSe.

(3) Fabrication process of GaSe/MoS_2 photodetector

Figure S3 depicts the preparation procedure of the GaSe/MoS_2 vdW heterostructure photodetector. The OM image of the GaSe nanosheet on the SiO_2 (300 nm)/Si substrate is presented in Figure S3(a). Note that the GaSe nanosheet is partially removed from the SiO_2/Si substrate after being spin-coated and peeled off with PPC, as demonstrated in Figure S3(b) for the remaining part of the GaSe sample. The AFM image of the remaining part of the GaSe nanosheet is shown in Figure S3(c). The height profile reveals that the GaSe nanosheet has a thickness of ~ 24.7 nm. The GaSe nanosheet was then transferred to the Au electrodes on the PET substrate, which is shown in Figure S3(d). The OM image of the MoS_2 nanosheet on the SiO_2 (300 nm)/Si substrate is presented in Figure S3(e). Figure S3(f) shows the AFM image of the MoS_2 nanosheet and the thickness of the MoS_2 nanosheet is ~ 170 nm. The fabrication of the GaSe/MoS_2 photodetector is achieved after the transfer of the MoS_2 nanosheet onto to the GaSe and Au electrodes on the PET substrate, which is presented in Figure 3c.

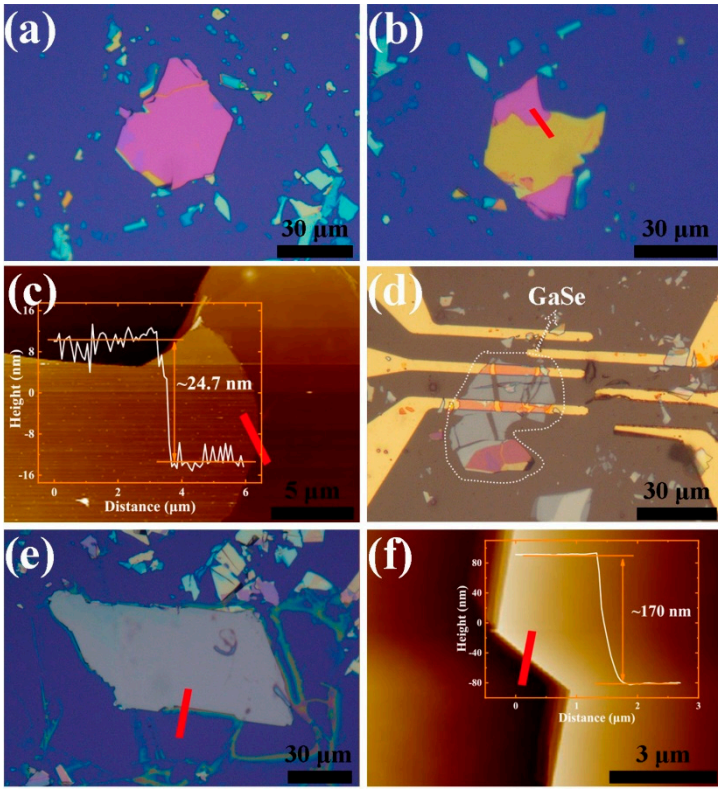

Figure S3. The fabrication process of the GaSe/MoS_2 vdW heterostructure photodetector. (a) OM image of the GaSe nanosheet on the SiO_2 (300 nm)/Si substrate. (b) OM image of the remaining sample after the GaSe nanosheet was removed with PPC. (c) AFM image of the remaining part of the GaSe nanosheet. Inset is the height profile. (d) OM image of the GaSe nanosheet transferred to the Au electrodes on PET substrate. (e) OM image of the MoS_2 nanosheet on the SiO_2 (300 nm)/Si substrate. (f) AFM image of the MoS_2 nanosheet. Inset is the height profile.

(4) Photoresponse of the GaSe photodetector

Figure S4(a) is the I-V curves of the GaSe photodetector in the dark and under 450 nm illumination with 0.36, 1.17 and 4.90 mW/mm^2 light power densities. These curves are comparable to the I-V curves in Figure 4a. In the meantime, the GaSe photodetector is sensitive to variations in light intensity. The number of photogenerated carriers and the current of the photodetector both increase as the light power density rises. Figure S4(b) depicts the single-cycle temporal photoresponse of the device at a bias of 2 V while switching 450 nm light with the light power density of 4.90 mW/mm^2. The device has a rapid response speed. In this case, the response time and recovery time are defined as the amount of time necessary for 10% of the photocurrent value to increase to 90% and for 90% of the photocurrent value to decrease to 10%, respectively. Consequently, both the response time and recovery time are 40 ms. It is notable that due to the accuracy of the measuring equipment, the response time and the recovery time were not precisely measured, and the actual values may be less than 40 ms.

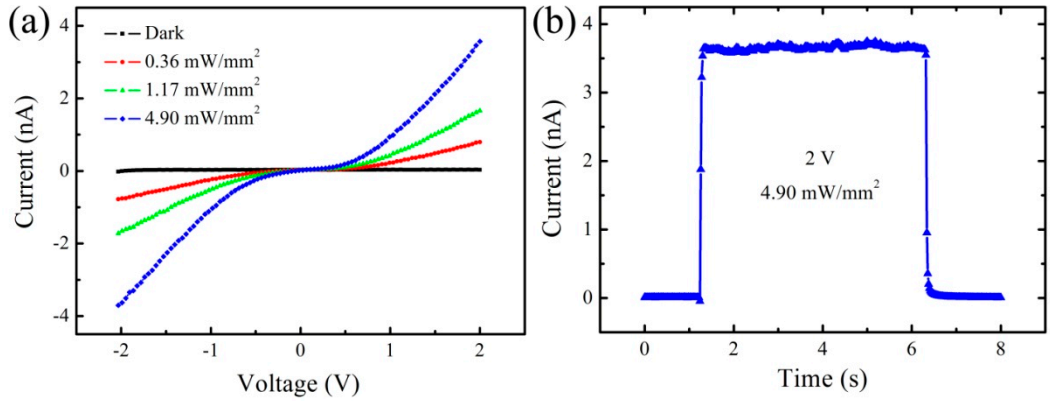

Figure S4. Photoresponse of the GaSe photodetector. (a) I-V curves in the dark and under 450 nm light illumination with different light power densities. (b) Single-cycle temporal photoresponse of the device at 2 V by switching 450 nm light with 4.90 mW/mm^2 light power density.

(5) Photoresponse of the MoS_2 photodetector

In Figure S5(a), the I-V curves of the MoS_2 photodetector are shown in the dark and under 450 nm light illumination with 0.36, 1.17 and 4.90 mW/mm^2 light power densities. These curves are similar to the I-V curves seen in Figure 5a. Additionally, the MoS_2 photodetector is sensitive to variations in light intensity. Figure S5(b) depicts the single-cycle temporal photoresponse of the device at a bias of 2 V while switching 450 nm light with the light power density of 4.90 mW/mm^2. The device also features a rapid response speed, with both the response time and recovery time being 40 ms.

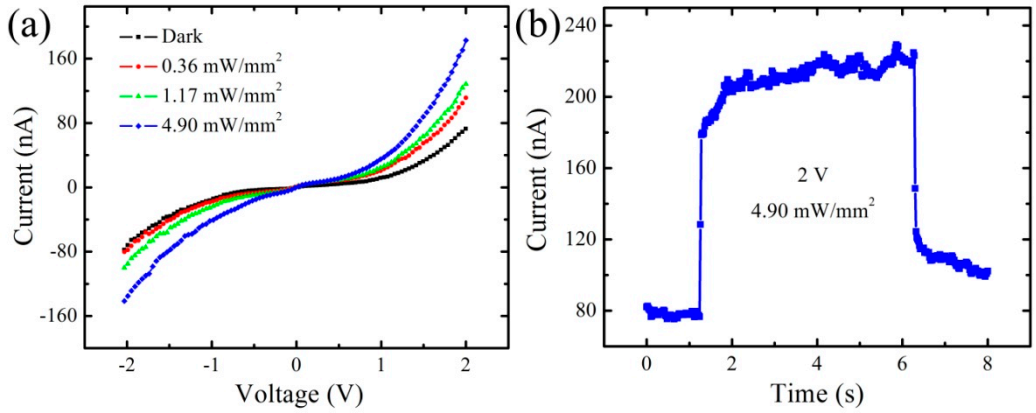

Figure S5. Photoresponse of the MoS_2 photodetector. (a) I-V curves in the dark and under 450 nm light illumination with different light power densities. (b) Single-cycle temporal photoresponse of the device at 2 V by switching 450 nm light with 4.90 mW/mm^2 light power density.

(6) Photoresponse of the GaSe/MoS_2 vdW heterojunction photodetector

Figure S6(a) depicts the I-V curves of the GaSe/MoS_2 vdW heterojunction photodetector in the dark and under 450 nm light illumination with 0.36, 1.17 and 4.90 mW/mm^2 light power densities. These curves are analogous to the I-V curves seen in Figure 6a. In addition,

the GaSe/MoS_2 vdW heterojunction photodetector exudes a high sensitivity to variations in light intensity. Figure S6(b) shows the single-cycle temporal photoresponse of the device at a bias of 2 V, switching 450 nm light with the light power density of 4.90 mW/mm^2. The GaSe/MoS_2 vdW heterojunction photodetector shows fast switching speed with a response time and recovery time of about 20 ms.

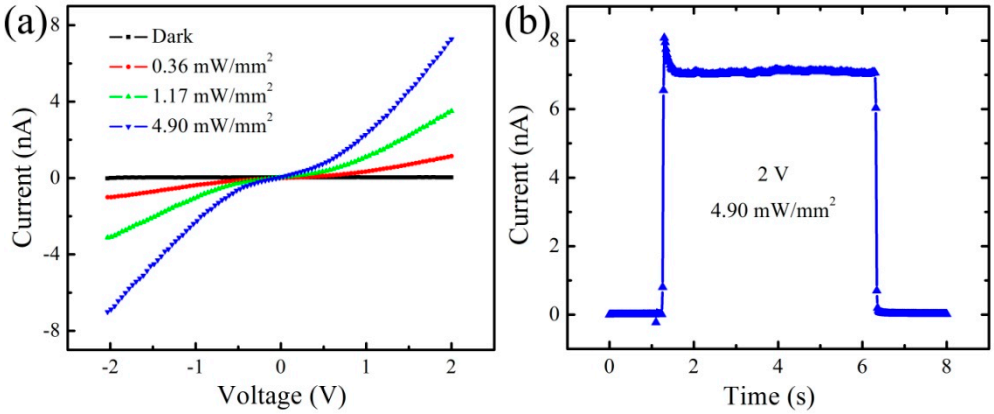

Figure S6. Photoresponse of the GaSe/MoS_2 vdW heterojunction photodetector. (a) I-V curves in the dark and under 450 nm light illumination with different light power densities. (b) Single-cycle temporal photoresponse of the device at 2 V by switching 450 nm light with 4.90 mW/mm^2 light power density.

(7) Comparison of photoelectric properties

The comparison table of photoelectric properties for individual Gase, MoS_2 and GaSe/MoS_2 vdW heterostructure including responsivity, on-off ratio, detectivity and response/recovery time is presented in Table S1.

Table S1. Comparison of photoelectric properties for individual GaSe, MoS_2 and GaSe/MoS_2 vdW heterostructure.

Type	Responsivity (mA W^{-1})	On-off ratio	Detectivity (Jones)	Response/Recovery time (ms)
GaSe	10.5	225	4.74×10^7	40/40
MoS_2	2496.8	2.3	1.07×10^8	40/40
GaSe/ MoS_2	22.6	380	8.54×10^7	20/20

(8) Comparison of photoelectric properties with those in other related literatures

The comparison of the photoelectric performances of the GaSe/MoS_2 heterostructure, individual MoS_2 and GaSe devices in this paper with those in other related literatures are listed in Table S2. The photodetectors in this work show comparable performances with those in the previous reported papers. It is notable that the photodetectors in this work are fabricated on the flexible PET substrates, showing the efficiency in the flexible situation compared with

other ones.

Table S2. Comparison of photoelectric performances with those in other related literatures.

Channel material	Wavelength (nm)	Responsivity (mA W^{-1})	Detectivity (Jones)	Response time	Ref.
GaSe/MoS_2	300	~60	/	80 ms	[3]
GaSe/ MoS_2	520	~670	~2.3×10^{11}	155 μs	[4]
GaSe/ MoS_2	520	~37	~1.9×10^{10}	620 μs	[4]
GaSe/ MoS_2	450	~900	6.5×10^{9}	5 ms	[5]
GaSe/ MoS_2	450	22.6	8.54×10^{7}	20 ms	This work
MoS_2 (40-60 nm)	532	~59000	/	42 μs	[6]
MoS_2 (~0.8 nm)	550	~7.5	/	50 ms	[7]
MoS_2 (~170 nm)	450	2496.8	1.07×10^{8}	40 ms	This work
GaSe (~4 nm)	254	~2800	/	20 ms	[8]
GaSe (~6 nm)	520	~2200	/	30 ms	[9]
GaSe (~24.7 nm)	450	10.5	4.74×10^{7}	40 ms	This work

(9) Stability of the GaSe/MoS_2 photodetector

In order to demonstrate the long-term stability of the GaSe/MoS_2 vdW heterojunction photodetector, we performed the photoelectric performance test for the device. Note that we measured the same photodetector twice. The pristine test was performed immediately after the fabrication of the device, while the secondary test was carried out after testing the device for a period of time under various testing environments. Figure S7(a) presents the comparison of I-V curves between a pristine test and a secondary test under the same incident light with the wavelength of 450 nm. Comparison of the temporal photoresponse for the two tests at a bias of 2 V by switching the incident light is shown in Figure S7(b). Compared with the pristine test of the device, the current under incident light shows a decreased trend during the secondary test, which may result from the increased defects during the measurement. Despite the decrease of current, the temporal photoresponse of the heterojunction device is distinct and stable by switching the incident light.

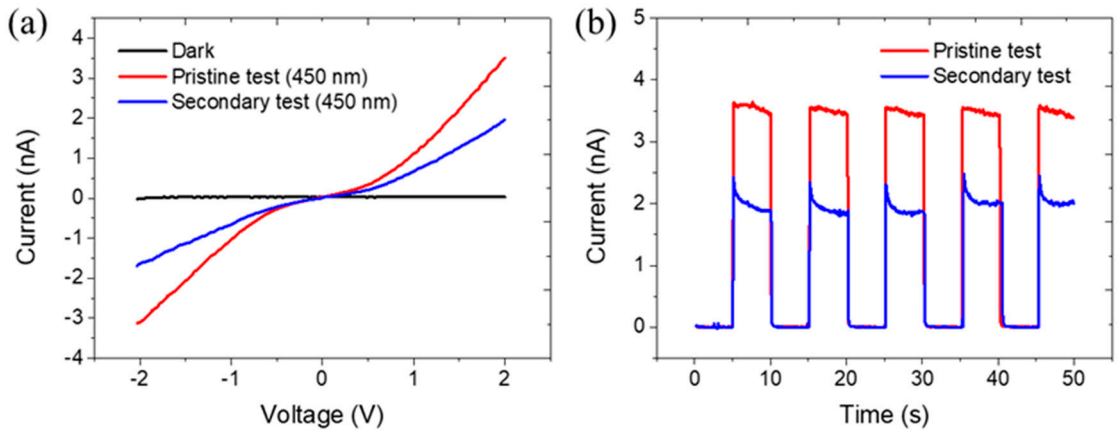

Figure S7. Stability of the GaSe/MoS_2 vdW heterojunction photodetector. (a) I-V curves in the dark and under incident light. (b) Temporal photoresponse of the heterojunction device at a bias of 2 V by switching 450 nm light.

References

1 Kwak, J. Y.; Hwang, J.; Calderon, B.; Alsalman, H.; Munoz, N.; Schutter, B.; Spencer, M. G. Electrical Characteristics of Multilayer MoS_2 FET's with MoS_2/Graphene Heterojunction Contacts. *Nano Letters* **2014**, *14*, 4511-4516.

2 Islam, A.; Lee, J.; Feng, P. X. L. Atomic Layer GaSe/MoS_2 van der Waals Heterostructure Photodiodes with Low Noise and Large Dynamic Range. *ACS Photonics* **2018**, *5*, 2693-2700.

3 Zhou, N.; Wang, R.; Zhou, X.; Song, H.; Xiong, X.; Ding, Y.; Lü, J.; Gan, L.; Zhai, T. P-GaSe/N-MoS_2 Vertical Heterostructures Synthesized by van der Waals Epitaxy for Photoresponse Modulation. *Small* **2018**, *14*, 1702731.

4 He, Z.; Guo, J.; Li, S.; Lei, Z.; Lin, L.; Ke, Y.; Jie, W.; Gong, T.; Lin, Y.; Cheng, T. *et al.* GaSe/MoS_2 Heterostructure with Ohmic-Contact Electrodes for Fast, Broadband Photoresponse, and Self-Driven Photodetectors. *Advanced Materials Interfaces* **2020**, *7*, 1901848.

5 Zou, Z.; Liang, J.; Zhang, X.; Ma, C.; Xu, P.; Yang, X.; Zeng, Z.; Sun, X.; Zhu, C.; Liang, D. *et al.* Liquid-Metal-Assisted Growth of Vertical GaSe/MoS_2 p–n Heterojunctions for Sensitive Self-Driven Photodetectors. *ACS Nano* **2021**, *15*, 10039-10047.

6 Tang, W.; Liu, C.; Wang, L.; Chen, X.; Luo, M.; Guo, W.; Wang, S.-W.; Lu, W. MoS_2 Nanosheet Photodetectors with Ultrafast Response. *Applied Physics Letters* **2017**, *111*, 153502.

7 Yin, Z.; Li, H.; Li, H.; Jiang, L.; Shi, Y.; Sun, Y.; Lu, G.; Zhang, Q.; Chen, X.; Zhang, H. Single-Layer MoS_2 Phototransistors. *ACS Nano* **2011**, *6*, 74-80.

8 Hu, P.; Wen, Z.; Wang, L.; Tan, P.; Xiao, K. Synthesis of Few-Layer GaSe Nanosheets for High Performance Photodetectors. *ACS Nano* **2012**, *6*, 5988-5994.

9 Huang, H.; Wang, P.; Gao, Y.; Wang, X.; Lin, T.; Wang, J.; Liao, L.; Sun, J.; Meng, X.; Huang, Z. *et al.* Highly Sensitive Phototransistor Based on GaSe Nanosheets. *Applied Physics Letters* **2015**, *107*, 143112.